

Electronic Supplementary Material (ESI)

For

**Novel electrochemical redox method for simultaneous recovery of
spent lithium-ion batteries cathodes and anodes**

Jiao Kong,^a Shiyu Zhou,^a Ting He,^a Shuai Gu^{*a, b} and Jianguo Yu^{*a, b}

^a *National Engineering Research Centre for Integrated Utilization of Salt Lake Resources, East China University of Science and Technology, Shanghai, 200237, China.*

^b *Joint International Laboratory for Potassium and Lithium Strategic Resources, East China University of Science and Technology, Shanghai, 200237, China.*

Table of Contents

Fig. S1. SEM-EDX images of the spent LIBs anode materials

Fig. S2. The flowchart of the graphite purification process

Table S1. Corrosion current (i_0), corrosion potential (E_c), and cathodic/ anodic charge transfer coefficient (α_c/α_a) at different acid concentrations

Fig.S3. Kinetic fitting of Li (a), Co (b), and Al (c) at -0.15 V, in the 0.5 M H₂SO₄ solution at different temperatures

Table S2. A comprehensive summary of the kinetic models

Fig.S4. SEM-EDX analysis of spent cathodes (a, b) and anodes (c, d).

Fig.S5. The leaching ratios of (a) Li, Mn, Al, (b) Co, Ni under the optimum conditions (-0.15 V, 0.5M H₂SO₄, 400 rpm, 30 °C)

Fig.S6. the cell potential comparison for Cu foil as the anode and titanium mesh as the anode.

Fig.S7. SEM-EDX images of the cathode residuals

Fig.S8. XPS survey(a) and the deconvoluted high-resolution XPS curves of Co 2p (b) and O 1s (c) of the cathode residuals

Fig.S9. Characterization of recovered conductive agent (a) SEM image, (b)size distributions

Fig.S10. SEM-EDX analysis of electrodeposited Cu

The calculation for life cycle and economic assessment

Fig.S11. System boundaries for LCA research of the proposed (a), and the conventional electrochemical process (b)

Table S3. EDX results of the spent LIBs cathode materials.

Table S4. EDX results of the spent LIBs anode materials.

Table S5. Material and energy input/output list

Table S6. Detailed energy input/output list

Table S7. CMP and data sources of each item

Table S8. The environmental impact of electricity in the electrochemical process proposed in this study and the traditional method

Table S9. The environmental impact of residue in the electrochemical process proposed in this study and the traditional method

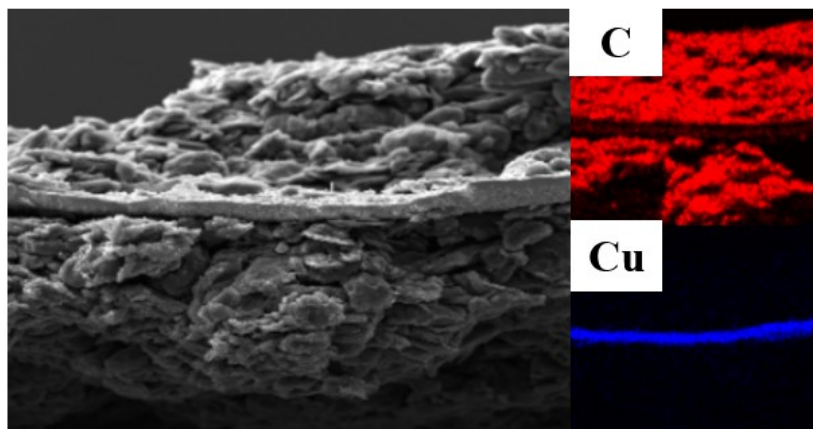


Fig. S1 SEM-EDX images of the spent LIBs anode materials.

The graphite recycled from the sulfuric acid solution

↓
Impurities removal with deionized water

↓
Binder removal with NMP

↓
Drying

The purified graphite

↓
Remanufacture of new anode material

Fig. S2 The flowchart of the graphite purification process.

Table S1 Corrosion current(i_0), corrosion potential (E_c), and cathodic/ anodic charge transfer coefficient (α_c/α_a) at different acid concentrations.

Condition	i_0 (A/cm ²)	E_c (V)	α_c	α_a
0.1M H ₂ SO ₄ +1.9M Na ₂ SO ₄	3.98*10 ⁻⁹	0.67	0.3323	0.6787
0.5M H ₂ SO ₄ + 1.5M Na ₂ SO ₄	3.16*10 ⁻⁷	0.76	0.2483	0.8074
1M H ₂ SO ₄ + 1M Na ₂ SO ₄	1*10 ⁻⁶	0.77	0.2814	0.7045
2M H ₂ SO ₄	1.25*10 ⁻⁶	0.81	0.1919	0.8153

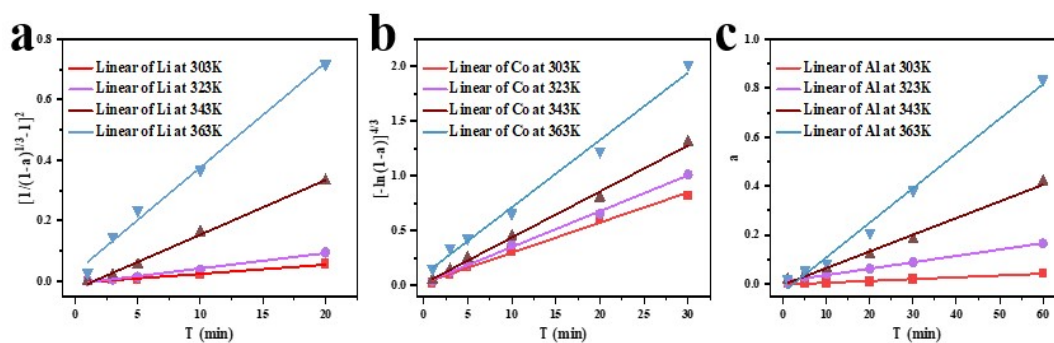


Fig.S3 Kinetic fitting of Li (a), Co (b), and Al (c) at -0.15 V, in the 0.5 M H₂SO₄ solution at different temperatures.

Table S2 A comprehensive summary of the kinetic models.

No.	Kinetic models	Name
D1	$kt = \alpha^2$	One-dimensional diffusion model
D2	$kt = (1-\alpha)\ln(1-\alpha)+\alpha$	Two-dimensional diffusion model
D3	$kt = [1-(1-\alpha)^{1/3}]^2$	Three-dimensional diffusion model (Jander)
D4	$kt = [1-(2\alpha/3)]-(1-\alpha)^{2/3}$	Ginstling-Brounshtein model
D5	$kt = [1/(1-\alpha)^{1/3}-1]^2$	Zhuravlev, Lesokhin and Templeman model
D6	$kt = [(1+\alpha)^{1/3}-1]^2$	Three-dimensional diffusion model (Anti- Jander)
D7	$k\ln t = [1-(1-\alpha)^{1/3}]^2$	Kroger and Ziegler model
D8	$kt = [1-(1-\alpha)^{1/2}]^2$	Cylindrical diffusion model (Jander)
D9	$kt = [1-(1+\alpha)^{1/2}]^2$	Cylindrical diffusion model (Anti-Jander)
D10	$kt = [1/((1-\alpha)^{1/3})]-1$	Dickinson and Heal model
D11	$kt = [1/((1-\alpha)^{1/3})]-1+1/3\ln(1-\alpha)$	Dickinson and Heal model
D12	$kt = 1/5(1-\alpha)^{-5/3}-1/4(1-\alpha)^{-4/3}+1/20$	Dickinson and Heal model
A1	$kt = [-\ln(1-\alpha)]^{1/4}$	Avrami-Erofeev model
A2	$kt = [-\ln(1-\alpha)]^{1/2}$	Avrami-Erofeev model
A3	$kt = [-\ln(1-\alpha)]^{1/3}$	Avrami-Erofeev model
A4	$kt = [-\ln(1-\alpha)]^{4/3}$	Avrami-Erofeev model
A5	$kt = [-\ln(1-\alpha)]^{2/3}$	Avrami-Erofeev model
A6	$\ln k+n\ln t = \ln[-\ln(1-\alpha)]$	Avrami-Erofeev model
F0	$kt = \alpha$	Zero order
F1	$kt = -\ln(1-\alpha)$	First order
F2	$kt = (1-\alpha)^{-1}$	Second order
R2	$kt = 1-(1-\alpha)^{1/2}$	Interface (contracting area)
R3	$kt = 1-(1-\alpha)^{1/3}$	Interface (contracting volume)
R4	$kt = 1-(1-\alpha)^{2/3}$	Interface
P1 (n=2)	$kt = \alpha^{1/2}$	Power law (half)
P2 (n=3)	$kt = \alpha^{1/3}$	Power law (third)
P3 (n=4)	$kt = \alpha^{1/4}$	Power law (quarter)
E1	$kt = \ln \alpha$	Exponential
E2	$kt = [-\ln(1-\alpha)]^2$	Exponential
B1	$kt = \ln[\alpha/(1-\alpha)]$	Prout-Tompkins model

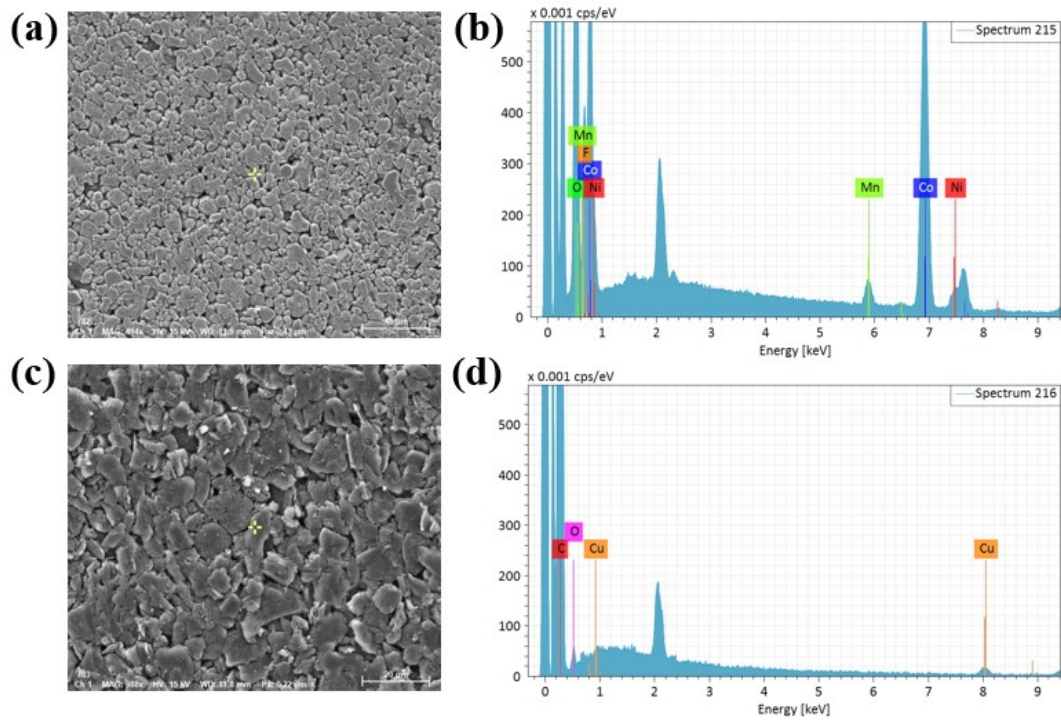


Fig.S4 SEM-EDX analysis of spent cathodes (a, b) and anodes (c, d).

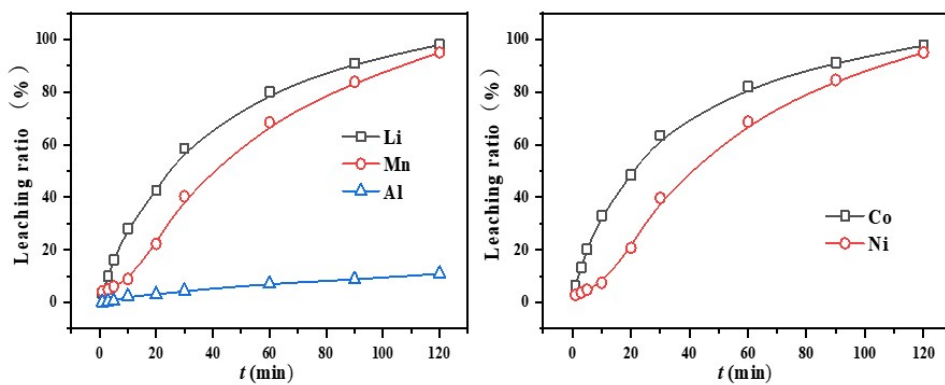


Fig.S5 The leaching ratios of (a) Li, Mn, Al, (b) Co, Ni under the optimum conditions (-0.15 V, 0.5M H₂SO₄, 400 rpm, 30 °C)

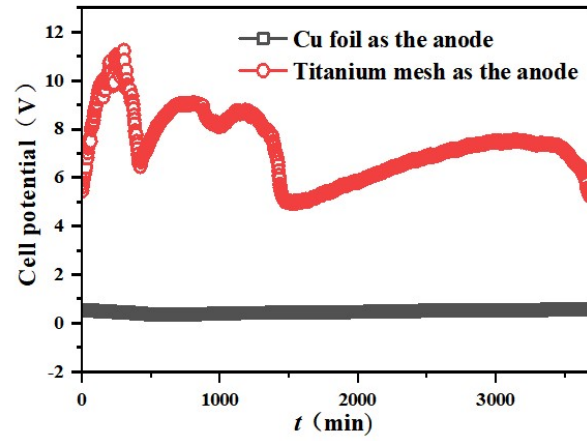


Fig. S6 the cell potential comparison for Cu foil as the anode and titanium mesh as the anode.

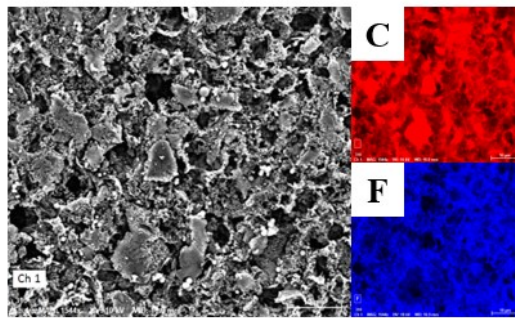


Fig.S7 SEM-EDX images of the cathode residuals.

Fig. S8a shows the cathode residuals mainly contain C (conductive agent and binder), F (residual electrolyte), Cu (Electrodeposition on the residuals), and Co (small amounts of unleached valued metals) elements. High-resolution and deconvoluted curves of Co (Fig. S8b) showed that $2p_{3/2}$ orbitals at 779.76 eV and 780.84 eV were attributed to Co_3O_4 and CoO , respectively, while the $2p_{1/2}$ orbitals at 794.76 eV and 796.09 eV were both attributed to Co_3O_4 , indicating two different existential status of cobalt in the leaching residual. Meanwhile, the O 1s orbitals (Fig. S8c) at 529.54 eV (CoO) and 532.74 eV (Co_3O_4), which verified the results of the peak fitting of Co elements.

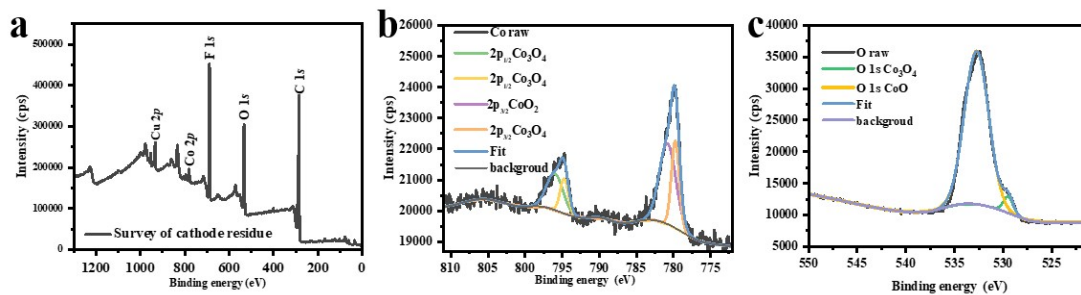


Fig.S8 XPS survey(a) and the deconvoluted high-resolution XPS curves of Co $2p$ (b) and O $1s$ (c) of the cathode residuals.

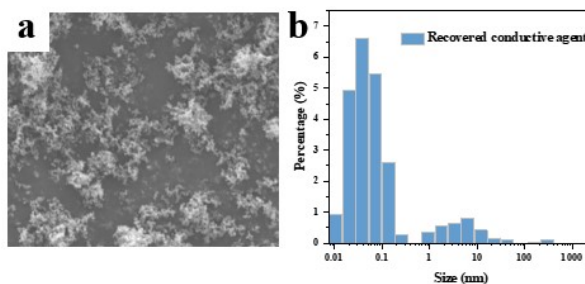


Fig.S9 Characterization of recovered conductive agent (a) SEM image, (b)size distributions.

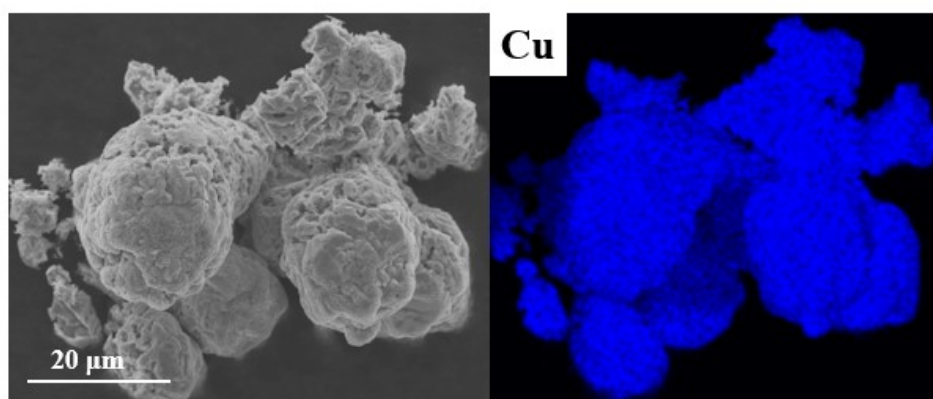


Fig.S10 SEM-EDX images of electrodeposited Cu.

Table S3 EDX results of the spent LIBs cathode materials.

Element	Norm. C (wt. %)	Atom. C (at. %)
Co	64.33	36.82
O	25.30	53.33
Ni	5.02	2.88
Mn	2.19	1.35
F	3.16	5.61

Table S4 EDX results of the spent LIBs anode materials.

Element	Norm. C (wt. %)	Atom. C (at. %)
C	95.35	97.72
O	2.40	1.85
Cu	2.25	0.44

The calculation for life cycle and economic assessment

The environmental impact of the proposed and conventional electrochemical process was obtained by SimaPro9 software based on the CML-IA baseline model. Fig.S11 shows the system boundary diagram of the electrochemical process.

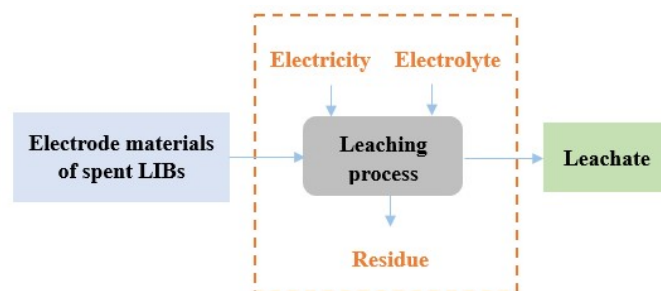


Fig.S11 System boundaries for LCA research of the electrochemical process.

Matter and energy inputs and outputs are listed according to the system boundary (Table S3). The data in Table S2 are based on the transfer of 50 mol of electrons (handling 1kg of cathode and 3.4kg of anode materials). To further compare the impact of electricity from the electrolysis, the evaluation was carried out again. A detailed energy list is shown in Table S4. The data in Table S4 are based on the 1kg of cathode materials. The electricity consumption of the process mainly comes from electrolysis and heating of the leaching solution, which is calculated according to Eq. (1~5).

$$Q = Q_t / \eta \quad (1)$$

$$Q_t = Q_h + Q_c \times t + Q_e \quad (2)$$

$$Q_h = mc\Delta T_1 \quad (3)$$

$$Q_c = \lambda A \Delta T_2 \quad (4)$$

$$Q_e = UIt \quad (5)$$

Where Q is electricity consumption in kJ; Q_t is the total energy consumption for time (t); η is the energy conversion efficiency of electricity to heat in this case 0.9; Q_h is the required energy for heating the solution to a certain temperature with the temperature difference (in K) in kJ; Q_c is the total energy loss by heat conduction caused by the temperature difference (in K) in kJ/h; Q_e is the required energy for electrolysis in kJ; m is the solution's mass in kg, c is the solution's specific heat capacity in kJ/(kg·K); λ is the container's heat transfer coefficient in kJ/(m²·K·h); A is the surface area of heat container in m²; U is the voltage during electrolysis; I is current during electrolysis.

Table S5 Material and energy input/output list.

	The proposed electrochemical process	The conventional electrochemical process
Input	H ₂ SO ₄ , 12.88 kg; H ₂ O, 268 kg; Electricity consumption, 4.2 kW·h	H ₂ SO ₄ , 12.88 kg; H ₂ O, 268 kg; Electricity consumption, 4.2 kW·h
Output	Residue, 0.2 kg	Residue, 3.6 kg

Table S6 Detailed energy input/output list.

	The proposed electrochemical process	The conventional electrochemical process
Input	Electricity consumption from the electrolysis, 163 J; Electricity consumption from the heating, 4.2 kW·h;	Electricity consumption from the electrolysis, 86.4 KJ; Electricity consumption from the heating, 123 kW·h;
Output	Residue, 0.2 kg	Residue, 0.2 kg

The economics of the proposed recycling route were evaluated with multiple parameters, i.e., leaching time (t), temperature (T), leaching ratio ($LR_{i(t,T)}$), reagents consumption leaching profit (P(t, T)), labor costs, and energy costs as shown in Eq.(6)-(8). Eq. (8) was used for the convenience of calculation, not the real profit since all leached metals were not recovered in metallic form.

$$C_e = Q \times P_e / 3600 \quad (6)$$

$$P = \sum LR_{i(t,T)} \times UP_i - C_l - \sum R_j \times UP_j - C_e \quad (7)$$

Where C_e is the cost of heating with electricity in USD; P_e is the local electricity price in USD/kWh; C_l is the labor cost in USD; UP_i and UP_j represent the commodity market prices (CMP) of the product i and reagent j in USD/g; R_j is reagents j's consumption quantity in g; P is the overall profit of leaching, which is calculated by subtracting the sum of labor costs, energy costs, reagents costs ($\sum R_j \times UP_j$) from the sum of leached critical metals prices ($\sum LR_{i(t,T)} \times UP_i$). CMP of each product and reagent were shown in Table S5.

Table S7 CMP and data sources of each item.

Items	CMP	Sources (Accessed on 2022/12/26)
H ₂ SO ₄	0.3 USD/Kg	https://www.made-in-china.com/video-channel/sjzxlwchem_cjpxkPZXIIhN_Sulfuric-Acid-Exporter-and-Supplier-Sulphuric-Acid-H2so4.html
Li metal	0.4207 USD/g	https://hq.smm.cn/new-energy/list/11036
Co metal	0.0467 USD /g	https://hq.smm.cn/new-energy/list/11008
Al metal	0.0027 USD /g	https://hq.smm.cn/aluminum/category/201102250311
Cu metal	0.0094 USD /g	https://hq.smm.cn/copper/list/178
Graphite	0.0077 USD /g	https://hq.smm.cn/new-energy/list/12028
NMP	20 USD/ Kg	https://www.echemi.com/searchGoods/pid_Seven17565-n-methyl-2-pyrrolidone.html
Time cost	3.4 USD/h	The minimum hourly wage in Shanghai, China in 2022: http://rsj.sh.gov.cn/txcgl_17550/20201016/t0035_1394758.html
Electricity	0.10342 USD/kWh	Electricity prices: https://www.globalpetrolprices.com/South-Korea/electricity_prices/ .

Table S8 The environmental impact of electricity in the electrochemical process proposed in this study and the traditional method.

	Impact category	ADP (fossil fuels)	GWP/kg CO ₂ eq	ODP/kg CFC-11 eq	HTP/kg 1,4-DB eq	MAE/kg 1,4-DB eq
This study	Electricity for electrolysis	3.8*10 ⁻⁴	3.52*10 ⁻⁵	1.67*10 ⁻¹²	1.44*10 ⁻⁵	0.06
	Electricity for heating	35.53	3.27	1.55*10 ⁻⁷	1.34	5359.72
Traditional method	Electricity for electrolysis	0.21	0.02	8.81*10 ⁻¹⁰	0.01	30.63
	Electricity for heating	1040.78	95.79	4.53*10 ⁻⁶	39.06	156963.27

Table S9 The environmental impact of residue in the electrochemical process proposed in this study and the traditional method.

	Impact category	ADP (fossil fuels)	GWP/kg CO ₂ eq	ODP/kg CFC-11 eq	HTP/kg 1,4-DB eq	MAE/kg 1,4-DB eq
This study	Residue	0.14	0.57	1.24*10 ⁻⁹	4.47	1102.59
Traditional method	Residue	2.55	10.24	2.24*10 ⁻⁸	80.55	19846.65